Covalent Functionalization of Single-Walled Carbon Nanotubes Alters Their Densities Allowing Electronic and Other Types of Separation

Woo-Jae Kim, Nitish Nair, Chang Young Lee, and Michael S. Strano*

Department of Chemical Engineering, Massachusetts Institute of Technology, Cambridge, Massachusetts 02139

Received: November 15, 2007; In Final Form: January 22, 2008

We show that covalently attached functional groups can alter the densities of individual single-walled carbon nanotubes (SWNTs) in a predictable and highly controllable manner. A volume-additivity model based on molecular group contributions can be used to estimate the density difference between 4-hydroxyphenyl-functionalized and nonfunctionalized HiPco SWNTs as approximately 98.3 kg/m^3, compared with 97.9 kg/m^3 measured by density-gradient centrifugation. Conversely, the estimated density difference between the (6,5) (0.75 nm diameter) and (9,8) (1.17 nm diameter) SWNTs is smaller at 23.4 kg/m^3. We conclude that covalent functionalization can provide an effective handle to separate particular SWNTs from a typical diameter distribution. We show that SWNT mixtures in which metallic SWNTs have been selectively reacted produce two distinct density fractions corresponding to functionalized metallic and pure semiconducting SWNTs. The results were confirmed by Raman spectroscopy, where the high-density fractions exhibit an increased disorder mode with a corresponding decrease in intensity for the low-density fraction. This method also allows for the first independent measure of (*n*,*m*) SWNTs having different chemical conversions with functional groups, which will allow for a more rigorous analysis of SWNT chemistry than is possible with uncalibrated spectroscopies such as Raman or photoluminescence.

1. Introduction

Separation and electronic sorting of single- or double-walled carbon nanotubes remain as substantial barriers to widespread electronic and optical applications of these materials.[1−3] The variations in electronic structure come from their unique 1-D tubular structure with various nanoscale diameters and chiralities, which are commonly defined by two integers (*n*,*m*).[4−6] When $n - m = 3q$ (where q is an integer), the SWNTs are metallic or semimetallic and when $n - m = q \pm 1$, the SWNTs are semiconducting.[7,8] There has been significant interest in separation of SWNTs by electronic type,[3,9−15] diameter,[16−18] and also length,[18] with progress made in the past 5 years. In the case of separation by electronic type, enrichment of metallic SWNTs has been achieved by dielectrophoresis,[9,19] and that of semiconducting SWNTs has been achieved by selective etching of metallic SWNTs through a gas-phase reaction.[14] Recently, density-gradient centrifugation[20] and free-solution electrophoresis[11] have demonstrated progress in the separation of both metallic and semiconducting SWNTs. All of these methods demonstrate high degrees of SWNT separation; however, they still have problems related to extension to all SWNT species and/or process scalability. We note that, despite this progress, these methods often apply only for SWNTs produced by specific preparations, e.g., CoMoCAT and laser ablation, or for those with a narrow range of chirality. Therefore, it is compelling to investigate a more generic separation method that would be valid for all types of SWNTs and a wide chirality range of separation.

In this work, we show for the first time that covalently attached functional groups can alter the densities of individual SWNTs, thereby allowing separation. A simple volume-additivity model is able to predict the density of SWNTs with given (*n*,*m*) values and their 4-hydroxyphenyl-functionalized analogues with reasonable accuracy. As a demonstration, we applied this concept to separate samples of SWNTs in which the metallic nanotubes had been selectively functionalized. We then verified the results by Raman and UV−vis−nIR absorption spectroscopies.

2. Experimental Methods

2.1. SWNT Preparation. As-prepared HiPco (i.e., prepared by the high-pressure carbon monoxide process; HPR 162.3 from Rice University) SWNTs were used for functionalization and separation, and no further purification procedure was performed to minimize side-wall functionalization. The SWNTs were suspended in H_2O using 2% (w/v) sodium cholate surfactants and sonicated, after which they were subjected to ultracentrifugation to disperse individually suspended SWNTs in an approach similar to that reported previously.[21] The final concentration of the SWNT solution was adjusted to be 0.005% (w/v).

2.2. Selective Functionalization. The 4-hydroxybenzene diazonium salt used as a reagent to attach 4-hydroxyphenyl chemical groups to the SWNTs was prepared by the reaction of nitrosonium tetrafluoroborate ($NOBF_4$) with 4-aminophenol ($HO-C_6H_4-NH_2$), as described previously.[11,22] Reaction of the SWNTs with the 4-hydroxybenzene diazonium salt was performed at 45 °C and pH 5.5 by injecting a diazonium salt solution into a reactor vessel containing the SWNTs using a syringe pump (Cole-Parmer). A total volume of 500 μL of the diazonium solution, with various concentrations, i.e., 0.42, 0.84, and 1.68 mM, was added at an injection rate of 20.83 μL/h into a total volume of 10 mL of SWNT solution.

* Corresponding author. E-mail: strano@mit.edu.

10.1021/jp710919b CCC: $40.75
Published on Web 04/18/2008

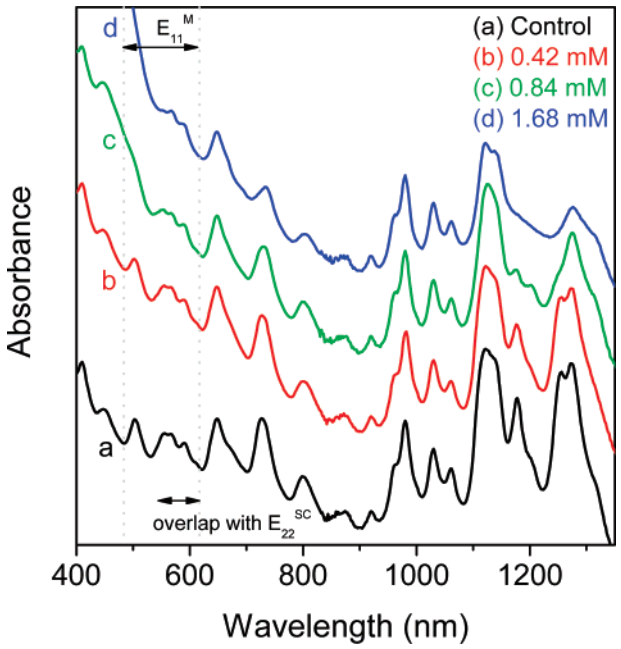

Figure 1. UV−vis−nIR absorption spectra of functionalized samples and the control as a reference. All spectra were offset with their original intensities maintained.

TABLE 1: Estimated Densities of Certain Nonfunctionalized and Functionalized SWNTs

		estimated density (kg/m^3)		
(*n*,*m*)	diameter (nm)	nonfunctionalized	functionalized	difference
(6,5)	0.75	1063.6	1157.8	94.2
(7,6)	0.89	1086.5	1182.8	96.3
(8,6)	0.96	1090.3	1188	97.7
(8,7)	1.03	1087.4	1187.1	99.7
(9,8)	1.17	1087	1190.6	103.6
measured average density (kg/m^3)		1089.6	1187.5	97.9

2.3. SWNT Separation Using Centrifugation. Separation of the SWNTs by density difference was performed using a density gradient in an approach similar to that described in the literature.[20] A density gradient was created using the non-ionic medium iodixanol [OptiPrep, 60% (w/v) iodixanol, Sigma-Aldrich]. The concentration of the initial gradient was adjusted to be 30% (w/v) with a volume of 7 mL and was positioned on top of a 60% (w/v) stop-layer solution having a volume of 3 mL. The rest of the tube was filled with water. One milliliter of SWNTs with a concentration of 32.5% (w/v) was injected at the bottom of the gradient, and the sample was centrifuged for 22 h at 22 °C and 32 000 rpm using a swinging-bucket rotor (SW 32.1 Ti, Beckman Coulter). The surfactant concentration was maintained at 2% (w/v) throughout the tube. SWNT samples were fractionated at every 150 μL after centrifugation using a fraction recovery system (Beckman Coulter) and characterized by UV−vis−nIR absorption spectroscopy (Shimadzu UV-310PC absorption spectrometer) and Raman spectroscopy (Kaiser Raman RXN1 analyzer).

3. Results and Discussion

3.1. Estimation of the Increase in SWNT Density Due to Functional Groups. We estimated the density difference between functionalized and nonfunctionalized SWNTs to investigate whether the increase in the density of the SWNTs by 4-hydroxyphenyl functional groups is sufficiently large enough to separate functionalized from nonfunctionalized SWNTs by density difference. First, the densities of SWNTs with various (*n*,*m*) values in SWNT−surfactant assemblies were calculated using a previously developed model.[23] We have shown that this representation faithfully predicts the results of quantitative ultracentrifugation for a large number of SWNTs. The density of the (*n*,*m*) SWNT−surfactant assembly ($\rho_{(n,m)}$) was calculated from the number of surfactant molecules adsorbed per unit length of the SWNTs (n_s). For a specific (*n*,*m*) SWNT, the number of carbons per nanometer (n_c) can be estimated,[24,25] which when combined with the number of surfactant molecules per nanometer (n_s) obtained in a previous study,[23] yields the following expression for the total mass per unit length ($M_{(n,m)}$)

$$M_{(n,m)} = n_s M_s + n_c M_c + n_f M_f + n_{sol} M_{sol} \quad (1)$$

where M_s (M_c) is the molecular (atomic) weight of a surfactant molecule (carbon atom). The last two terms are applicable when the interior of the SWNTs is filled with either n_f molecules (per nanometer) of air with a molecular weight of M_f or n_{sol} molecules (per nanometer) of water with a molecular weight of M_{sol}. The general formula for the volume per unit length of the assembly is

$$V_{(n,m)} = n_s V_s + \frac{\pi}{4} d_{eff}^{\ 2} - n_{sol} V_{sol} \quad (2)$$

$$d_{eff} = d_{(n,m)} + 2r_c \quad (3)$$

where r_c is the van der Waals radius of a carbon atom in aromatic molecules (~1.72 Å).[26] The third term in eq 2 is a correction when the interior of the SWNTs is accessible to water molecules whose molecular volume is V_{sol}. In this work, we assumed that the pores in the SWNT lattice were devoid of any fluid, i.e., $n_f = n_{sol} = 0$. The anhydrous molecular volume of a sodium cholate surfactant molecule used in this study (V_s) can be found in the literature.[27−29] However, anhydrous surfactant molecules impart little buoyancy to the nanotubes. Therefore, we accounted for one hydration shell when calculating the apparent molecular volume of sodium cholate (~1018 Å^3/molecule) using an approximate hydration number of 16.[30,31] Finally, the buoyant density of a generic nanotube is given by

$$\rho_{(n,m)} = \frac{M_{(n,m)}}{V_{(n,m)}} \quad (4)$$

We calculated the densities of five different SWNTs, i.e., (6,5), (7,6), (8,6), (8,7), and (9,8), with diameters ranging from 0.75 to 1.17 nm, as listed in Table 1. The estimated values vary from 1063.6 kg/m^3 for (6,5) SWNTs to 1087 kg/m^3 for (9,8) SWNTs, depending on the SWNT diameter. Because the typical diameter distribution of HiPco SWNTs falls into this range, i.e., from 0.75 to 1.17 nm, the density difference of 23.4 kg/m^3 among listed HiPco SWNTs can be considered a maximum difference expected for HiPco SWNTs. We reasoned that, if the density increase of the SWNTs upon the addition of functional groups is greater than 23.4 kg/m^3, then the functionalized SWNTs could be separated from nonfunctionalized SWNTs.

The densities of SWNTs functionalized with 4-hydroxyphenyl groups were also calculated for each (*n*,*m*) SWNT. The molecular mass and apparent molecular volume (105.3 Å^3/molecule)[32] of the 4-hydroxyphenyl group was included to the SWNT−surfactant system to calculate the densities of the

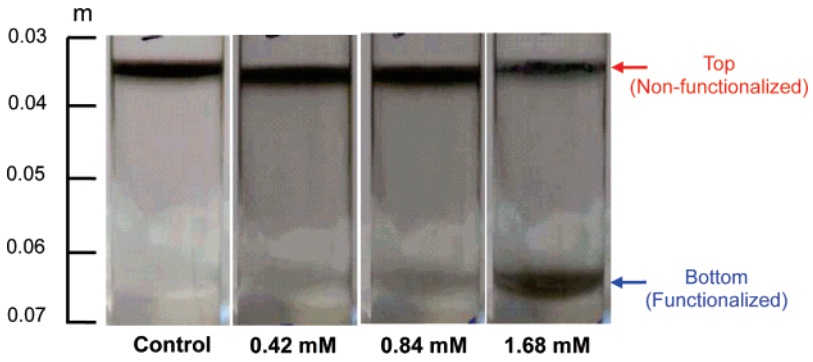

Figure 2. Pictures of four samples after 22 h of centrifugation. Locations of the top (density = 1089.6 kg/m^3) and bottom (density = 1187.5 kg/m^3) fractions are marked.

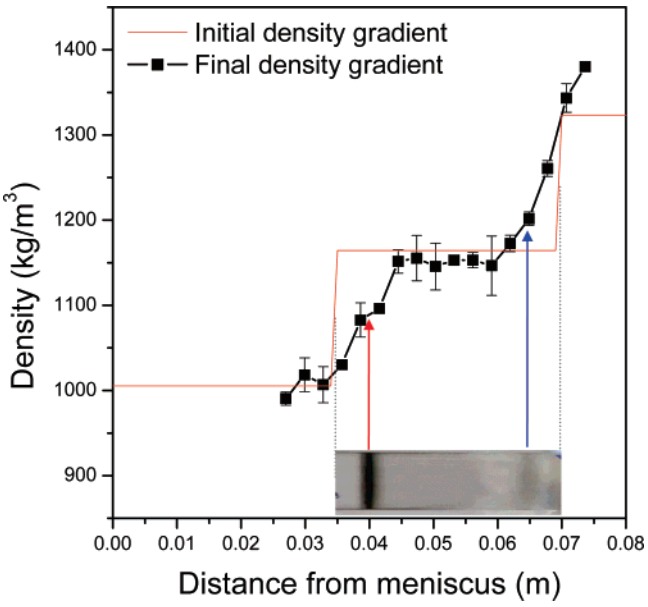

Figure 3. Density measurements of functionalized and nonfunctionalized SWNTs: initial density-gradient profile (red line), final density-gradient profile after 22 h of centrifugation (black line). The inset shows a picture of the centrifuge tube of the 0.84 mM reaction sample after centrifugation.

functionalized SWNTs. The number of functional groups per carbon atom was estimated to be 0.1, based on 0.42 mM diazonium concentration of this study, where all the injected reagents are reacted, leaving no residual in solution. Details of this estimation are presented in the Supporting information (Figure S1). We also assumed that the number of surfactant molecules per unit length was not influenced by the attachment of functional groups, because the apparent molecular volume of the functional group (105.3 Å^3/molecule) is ~10 times smaller than that of a surfactant molecule (1018 Å^3/molecule). The densities of various functionalized (*n*,*m*) SWNTs were estimated according to these assumptions and are listed in Table 1. The estimated density difference between the functionalized and nonfunctionalized SWNTs ranges from 94.2 for (6,5) SWNTs to 103.6 kg/m^3 for (9,8) SWNTs, greater than the 23.4 kg/m^3 maximum density difference for SWNTs with diameters in the 0.75−1.17 nm range. On the basis of these findings, we concluded that the density increase of SWNTs resulting from the attachment of functional groups is large enough for functionalized SWNTs to be separated from nonfunctionalized SWNTs using density-gradient-induced centrifugation.

3.2. Selective Functionalization. Three different samples of functionalized SWNTs were prepared, in which a small amount of metallic SWNTs, mostly metallic SWNTs, and a portion of large-diameter semiconducting SWNTs in addition to metallic SWNTs were reacted. Figure 1 shows the UV−vis−nIR absorption spectra of the three functionalized SWNT samples, obtained upon injection of 0.42, 0.84, and 1.68 mM reagent solutions, together with that of nonfunctionalized SWNTs (control) as a reference. For the 0.42 mM reagent solution (Figure 1b), the peak intensities representing the first van Hove transition of metallic species (E_{11}^M, 485−620 nm) start to decrease as compared to those of the nonfunctionalized SWNTs (control, Figure 1a), whereas the peak intensities representing the second (E_{22}^S, 620−900 nm) and first (E_{11}^S, 900−1350 nm) van Hove transitions of the semiconducting species scarcely change. These results indicate that the metallic SWNTs begin to selectively react with the functionalization reagent in preference to the semiconducting SWNTs, as reported previously.[2,22,33] At 0.84 mM reagent concentration (Figure 1c), small-diameter metallic SWNTs react completely because of the high reactivity originating from their large curvature.[2] At the highest reagent concentration, i.e., 1.68 mM (Figure 1d), some of the semiconducting SWNTs having a large diameter (1150−1350 nm) as well as all of the metallic SWNTs react. The peaks observed in the 520−620 nm region in Figure 1d originate from the E_{22}^S transition, rather than E_{11}^M transition, because the metallic SWNTs react at a higher rate than the semiconducting SWNTs in this reaction system.[22]

3.3. Separation of Functionalized from Nonfunctionalized SWNTs. The functionalized SWNTs prepared as described in the previous section and the control were centrifuged for 22 h in the density-gradient solution. Pictures of the centrifuge tubes of these four samples after centrifugation are presented in Figure 2. Except for the control sample, the injected SWNTs were consistently separated into two distinct fractions after centrifugation: one close to the top of the gradient solution (red) and one close to the bottom of the gradient solution (blue). The concentration of the bottom fraction increased (from 0.42 to 1.68 mM) as the extent of functionalization increased. Judging from the absence of a higher-density fraction in the control and its increasing concentration with reaction, we assigned this bottom band to fully 4-hydroxyphenylated SWNTs.

To verify that the density of SWNTs collected at the bottom of the centrifuge tubes was similar to the value estimated for the functionalized SWNTs as described in the previous section, actual densities of the top and bottom SWNTs were measured and compared with the estimated values in the case of the 0.84 mM reaction sample, and the results are shown in Figure 3. The inset in Figure 3 shows the actual picture of the 0.84 mM reaction sample after centrifugation (the same picture as in Figure 2). We calculated the average densities of the top and bottom fractions by matching the distance of each fraction from the meniscus with the final density of the solution. The average

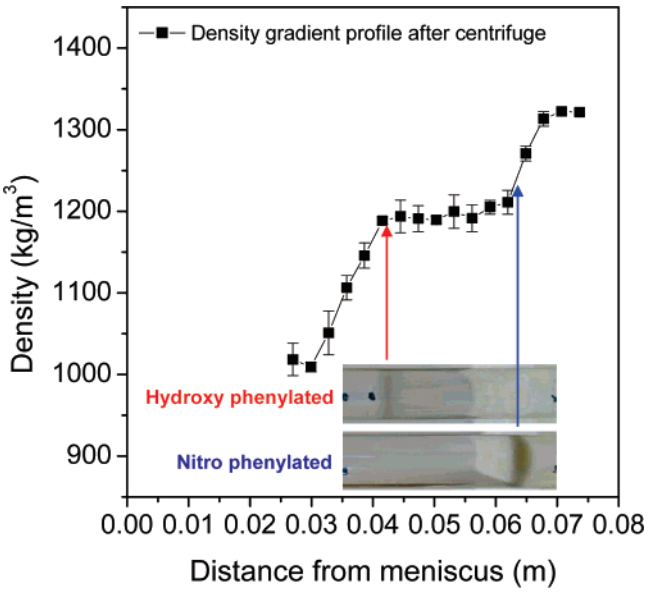

Figure 4. Density measurements of hydroxyphenylated and nitrophenylated SWNTs. The initial density gradient was adjusted to be 35% (w/v) iodixanol in water. Both SWNTs are fully functionalized.

measured densities for these fractions were 1089.6 and 1187.5 kg/m^3 (average estimated values for these fractions were 1082.9 and 1181.3 kg/m^3), respectively, giving a density difference between the two fractions of 97.9 kg/m^3, which is comparable to the calculated average density difference of 98.3 kg/m^3. This close agreement (within less than 1% error range) suggests that the bottom fraction is the functionalized SWNTs and the top fraction is the nonfunctionalized SWNTs.

There is a possibility that functionalized SWNTs could form bundles leading to higher densities, which would show results similar to the current separation. To clarify that the current separation originated from the increase in density resulting from the addition of functional groups rather than from bundling, we investigated whether there was a difference between the densities of SWNTs functionalized by different types of functional groups. The para-nitrophenyl group was chosen as a comparison, because the average estimated density for 4-nitrophenyl-functionalized SWNTs by the volume-additivity model is 1236.5 kg/m^3, which is higher than that of 4-hydroxyphenyl-functionalized SWNTs, i.e., 1181.3 kg/m^3. The concentration of the initial density gradient is adjusted to be 35% (w/v), rather than 30% (w/v), so that the two functionalized SWNTs would be spatially separated. Figure 4 shows the final density gradient together with pictures of the 4-hydroxy- and 4-nitrophenylated SWNTs in the centrifuge tubes after separation. The density of the 4-nitrophenyl-functionalized SWNTs is clearly higher than that of the 4-hydroxyphenyl-functionalized SWNTs, and the average measured density (1230.8 for the 4-nitrophenyl-functionalized SWNTs, compared to 1187.7 kg/m^3 for the 4-hydroxyphenyl-functionalized SWNTs) is in good agreement with the estimated value. The fact that the density of the functionalized SWNTs varies depending on the type of functional group, together with the fact that both the functionalized and nonfunctionalized SWNTs maintain their own densities irrespective of the density-gradient profiles (Figure S2), indicates that the separation of the current study originates from the density increase resulting from the addition of functional groups, rather than from aggregation or other interparticle influences.

We also performed UV−vis−nIR absorption and Raman measurements for the separated fractions to spectroscopically investigate the separation efficiency and purity. First, we tracked the disorder mode (D peak, 1305 cm^{-1}) and the tangential mode (G peak, 1592 cm^{-1}) for all separated fractions using 632.8 nm excitation to investigate the extent of functionalization in each fraction.[34] The results are shown in Figure 5, together with the data for each initial SWNT sample before separation. The insets in Figure 5 show pictures of the centrifuge tubes of the SWNT samples before and after separation. All of the Raman spectra in Figure 5 were normalized to the G peak to compare the D peak of each fraction, before and after separation. For the Raman spectra of the initial SWNT samples (black lines), the D peak intensity increases as the extent of reaction increases from the 4.2 mM reaction sample (Figure 5A) to the 16.8 mM reaction sample (Figure 5C), as anticipated from the UV−vis−nIR absorption results shown in Figure 1. After separation, noticeable changes in the D peak intensities are observed. The intensities of the D peaks of all bottom fractions (blue lines) increase and those of the top fractions (red lines) decrease compared to those of the initial reaction samples. This indicates that the functionalized SWNTs are separated from the mixtures and collected at the bottom and the nonfunctionalized SWNTs are also separated and collected at the top. The measurements are consistent with a separation based on the increase in density

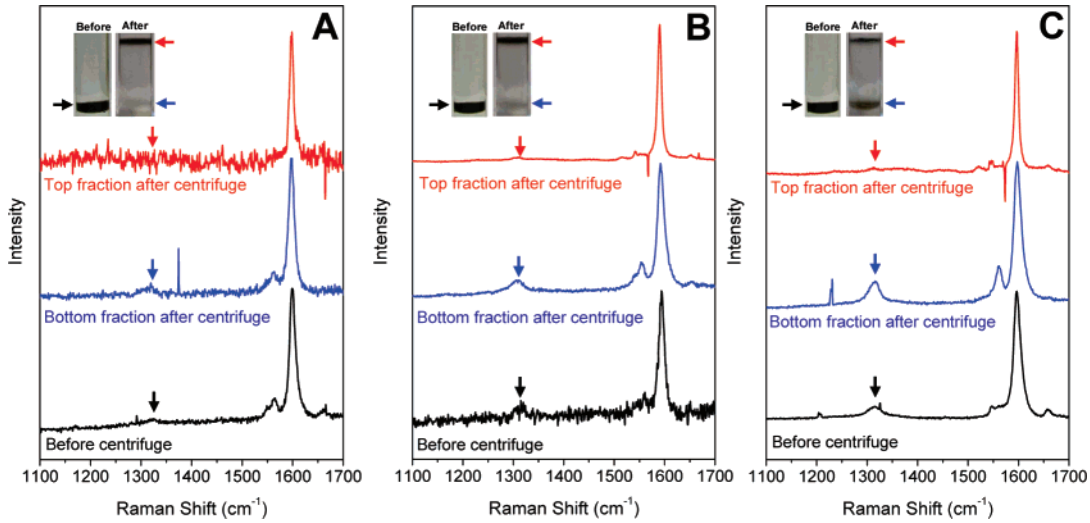

Figure 5. Raman excitation measurements (632.8 nm) for separated fractions and initial samples for three functionalized SWNTs: (A) 0.42, (B) 0.84, and (C) 1.68 mM.

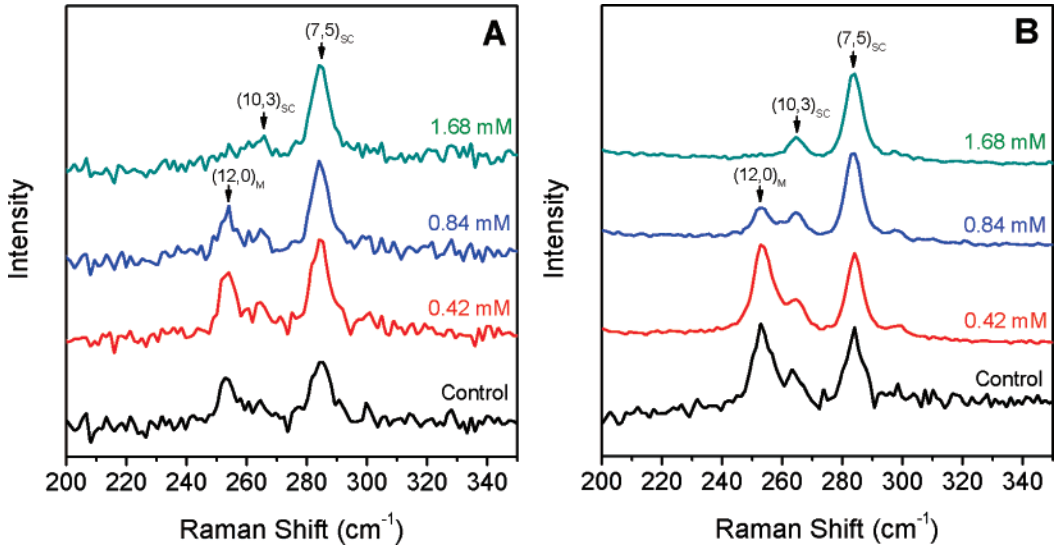

Figure 6. Radial breathing modes (RBMs) upon 632.8 nm Raman excitation for the (A) original reaction samples and (B) top fractions of separated samples.

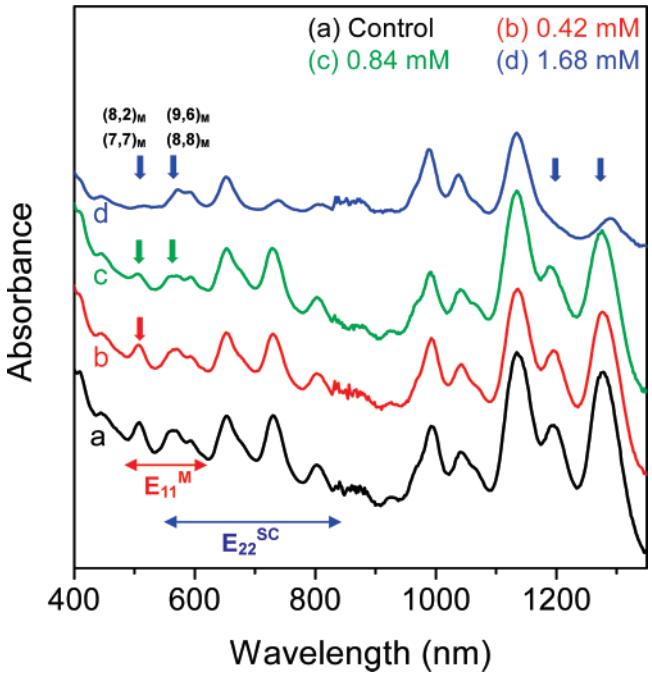

Figure 7. UV−vis−nIR absorption spectra of separated top fractions. All spectra were offset with their original intensities maintained.

resulting from the covalent attachment of the 4-hydroxyphenyl functional group.

We also observed the radial breathing modes (RBMs) of the separated fractions and the initial SWNT samples to investigate electronic-type separation, using 632.8 nm laser excitation, as both metallic and semiconducting SWNTs are in resonance at this wavelength. Figure 6A and 6B shows the RBMs of the initial SWNT samples and the separated top fractions, respectively. In Figure 6A, the RBM of the metallic SWNTs [(12,0)] decays as the reagent concentration increases, whereas those of the semiconducting SWNTs [(10,3) and (7,5)] scarcely change. The decay of RBM of the metallic SWNTs originates from the covalent functionalization of the metallic SWNTs with hydroxyphenyl groups,[2] and the extent of decay corresponds to the extent of reaction of the metallic SWNTs shown in Figure 1. The corresponding RBMs of the separated top fractions (Figure 6B) show similar behavior. However, the intensity decay of the RBMs of the metallic SWNTs in this case is not due to the covalent functionalization, because these fractions are free from functionalization as confirmed by the absence of the D peak in the Raman measurements (Figure 5). Therefore, the intensity decay of the metallic SWNTs represents an actual deficiency of metallic SWNTs in the separated top fractions, as the metallic SWNTs were functionalized and then removed from the top fraction during centrifugation. For the 16.8 mM reaction sample, in which all of the metallic SWNTs had completely reacted and been removed by centrifugation, only pure semiconducting SWNTs are present in the top fraction.

Furthermore, this method can be used to separate metallic SWNTs by diameter. Figure 7 shows the UV−vis−nIR absorption spectra of the nonfunctionalized top fractions. The arrows indicate the peak locations of the functionalized SWNTs, which thus removed from the top fraction and collected at the bottom fraction. In the 4.2 mM reaction sample (Figure 7b), only (8,2) and (7,7) metallic species, which have small diameters, have been removed, suggesting that pure (8,2) and (7,7) metallic SWNTs are separated and collected in the bottom fraction (Figure 2b). For the 8.4 mM reaction sample (Figure 7c), some of (9,6) and (8,8) metallic species, with large diameters, are also removed and collected in the bottom fraction (Figure 2c). These results suggest that further separation of metallic species by diameter can be achieved by controlling the reaction selectivity and successive separation. We note that this method also allows for the first independent measure of (*n*,*m*) SWNTs having different chemical conversions with functional groups, which will allow for a more rigorous analysis of SWNT chemistry than is possible with uncalibrated spectroscopies such as Raman or photoluminescence.

4. Conclusions

We show that covalently attached functional groups to SWNT alter their densities, thus enabling the separation of functionalized from nonfunctionalized SWNTs, as confirmed by density estimations using the volume-additivity model and actual demonstration of separation using 4-hydroxyphenyl functional groups. We also demonstrate the electronic-type separation of SWNTs and propose the possibility of separating metallic SWNTs by diameter, by controlling the reaction selectivity for metallic SWNTs.

Acknowledgment. We acknowledge a Class A grant from the Intel Corporation. M.S.S. appreciates an NSF-Career Award and a grant from the ACS-PRF for the support of this research. W-J.K. is grateful for support by a Korea Research Foundation Grant funded by the Korean Government (MOEHRD) (KRF-2005-214-D00260).

Supporting Information Available: Estimation of the number of 4-hydroxyphenyl functional groups per carbon atom and separation of functionalized SWNTs using different density-gradient profile. This material is available free of charge via the Internet at http://pubs.acs.org.

References and Notes

(1) Avouris, P. *Acc. Chem. Res.* **2002**, *35*, 1026.
(2) Strano, M. S.; Dyke, C. A.; Usrey, M. L.; Barone, P. W.; Allen, M. J.; Shan, H. W.; Kittrell, C.; Hauge, R. H.; Tour, J. M.; Smalley, R. E. *Science* **2003**, *301*, 1519.
(3) Krupke, R.; Hennrich, F.; von Lohneysen, H.; Kappes, M. M. *Science* **2003**, *301*, 344.
(4) McEuen, P. L. *Phys. World* **2000**, *13*, 31.
(5) Tans, S. J.; Devoret, M. H.; Groeneveld, R. J. A.; Dekker, C. *Nature* **1998**, *394*, 761.
(6) Frank, S.; Poncharal, P.; Wang, Z. L.; Heer, W. A. *Science* **1998**, *280*, 1744.
(7) Bronikowski, M. J.; Willis, P. A.; Colbert, D. T.; Smith, K. A.; Smalley, R. E. *J. Vac. Sci. Technol. A* **2001**, *19*, 1800.
(8) Reich, S.; Thomsen, C. *Phys. Rev. B* **2000**, *62*, 4273.
(9) Peng, H.; Alvarez, N. T.; Kittrell, C.; Hauge, R. H.; Schmidt, H. K. *J. Am. Chem. Soc.* **2006**, *128*, 8396.
(10) Baik, S. H.; Usrey, M. L.; Rotkina, L.; Strano, M. S. *J. Phys. Chem. B* **2004**, *108*, 15560.
(11) Kim, W. -J.; Usrey, M. L.; Strano, M. S. *Chem. Mater.* **2007**, *19*, 1571.
(12) Chattopadhyay, D.; Galeska, L.; Papadimitrakopoulos, F. *J. Am. Chem. Soc.* **2003**, *125*, 3370.
(13) Chen, Z.; Du, X.; Du, M.; Rancken, C.; Cheng, H.; Rinzler, A. *Nano Lett.* **2003**, *3*, 1245.
(14) Zhang, G.; Qi, P.; Wang, X.; Lu, Y.; Li, X.; Tu, R.; Bangsaruntip, S.; Mann, D.; Zhang, L.; Dai, H. *Science* **2006**, *314*, 974.
(15) Collins, P. G.; Arnold, M. S.; Avouris, P. *Science* **2001**, *292*, 706.
(16) Arnold, M. S.; Stupp, S. I.; Hersam, M. C. *Nano Lett.* **2005**, *5*, 713.
(17) Zheng, M.; Jagota, A.; Semke, E. D.; Diner, B. A.; McLean, R. S.; Lustig, S. R.; Richardson, R. E.; Tassi, N. G. *Nat. Mater.* **2003**, *2*, 338.
(18) Heller, D. A.; Mayrhofer, R. M.; Baik, S.; Grinkova, Y. V.; Usrey, M. L.; Strano, M. S. *J. Am. Chem. Soc.* **2004**, *126*, 14567.
(19) Hennrich, F.; Krupke, R.; Kappes, M. M.; Lohneysen, H. V. *J. Nanosci. Nanotechnol.* **2005**, *5*, 1166.
(20) Arnold, M. S.; Green, A. A.; Hulvat, J. F.; Stupp, S. I.; Hersam, M. C. *Nature Mater.* **2006**, 1, 60.
(21) O'Connell, M. J.; Bachilo, S. M.; Huffman, C. B.; Moore, V. C.; Strano, M. S.; Haroz, E. H.; Rialon, K. L.; Boul, P. J.; Noon, W. H.; Kittrell, C.; Ma, J. P.; Hauge, R. H.; Weisman, R. B.; Smalley, R. E. *Science* **2002**, *297*, 593.
(22) Nair, N.; Kim, W.-J.; Usrey, M. L.; Strano, M. S. *J. Am. Chem. Soc.* **2007**, *129*, 3946.
(23) Nair, N.; Kim, W.-J.; Braatz, R.; Strano, M. *Langmuir*, in published online Jan 23, 2008, http://dx.doi.org/10.1021/la702516u.
(24) Cabria, I.; Mintmire, J. W.; White, C. T. *Phys. Rev. B* **2003**, *67*, 121406.
(25) Saito, R.; Dresselhaus, G.; Dresselhaus, M. S. *Physical Properties of Carbon Nanotubes*; Imperial College Press: London, 1998.
(26) Kitaigorodskii, A. I. *Org. Kristallokhim.* **1955**, 558.
(27) Collins, G. L.; Motarjemi, M.; Jameson, G. J. *J. Colloid Interface Sci.* **1978**, *63*, 69.
(28) Horvath-Szabo, G.; Hoiland, H. *Langmuir* **1998**, *14*, 5539.
(29) Smith, W. B.; Barnard, G. D. *Can. J. Chem.* **1981**, *59*, 1602.
(30) Hayter, J. B.; Penfold, J. *Colloid Polym. Sci.* **1983**, *261*, 1022.
(31) Messina, P.; Morini, M. A.; Schulz, P. C. *Colloid Polym. Sci.* **2003**, *281*, 695.
(32) Ammon, H. L.; Mitchell, S. *Propellants, Explos., Pyrotech.* **1998**, *23*, 260.
(33) Usrey, M. L.; Lippmann, E. S.; Strano, M. S. *J. Am. Chem. Soc.* **2005**, *127*, 16129.
(34) Dillon, A. C.; Parilla, P. A.; Alleman, J. L.; Gennett, T.; Jones, K. M.; Heben, M. J. *Chem. Phys. Lett.* **2005**, *401*, 522.